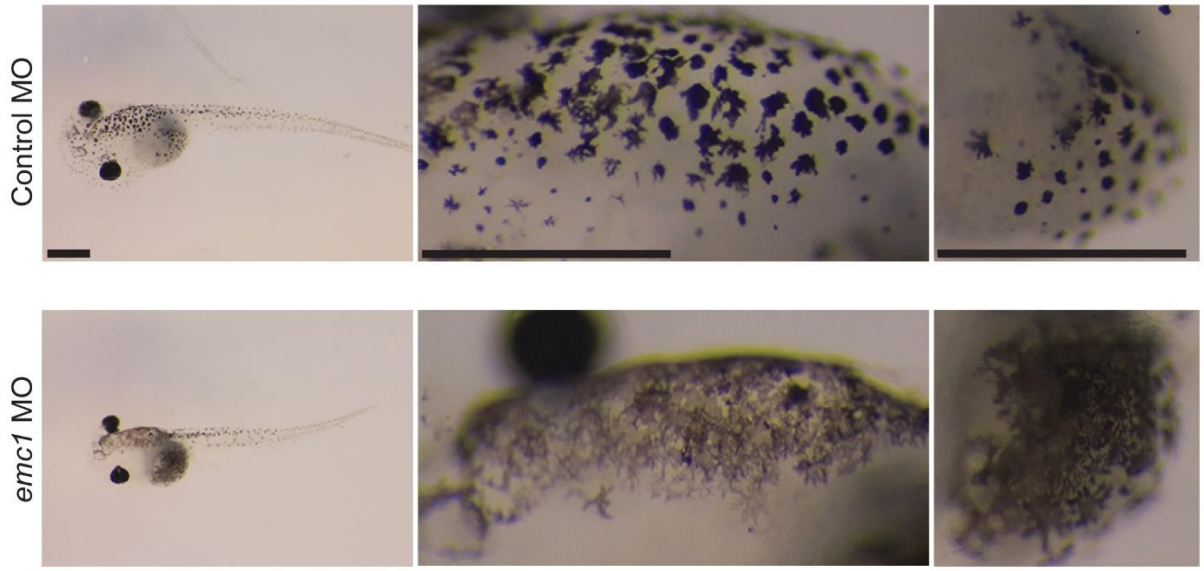

Supplemental Figure 1 Knockdown of *emc1* causes abnormal pigment cell morphology. Representative images of control MO and *emc1* MO injected stage 45 embryo pigment cell morphology. 30 embryos were imaged for each condition over 3 biological replicates. Scale bar indicates 500 μm.

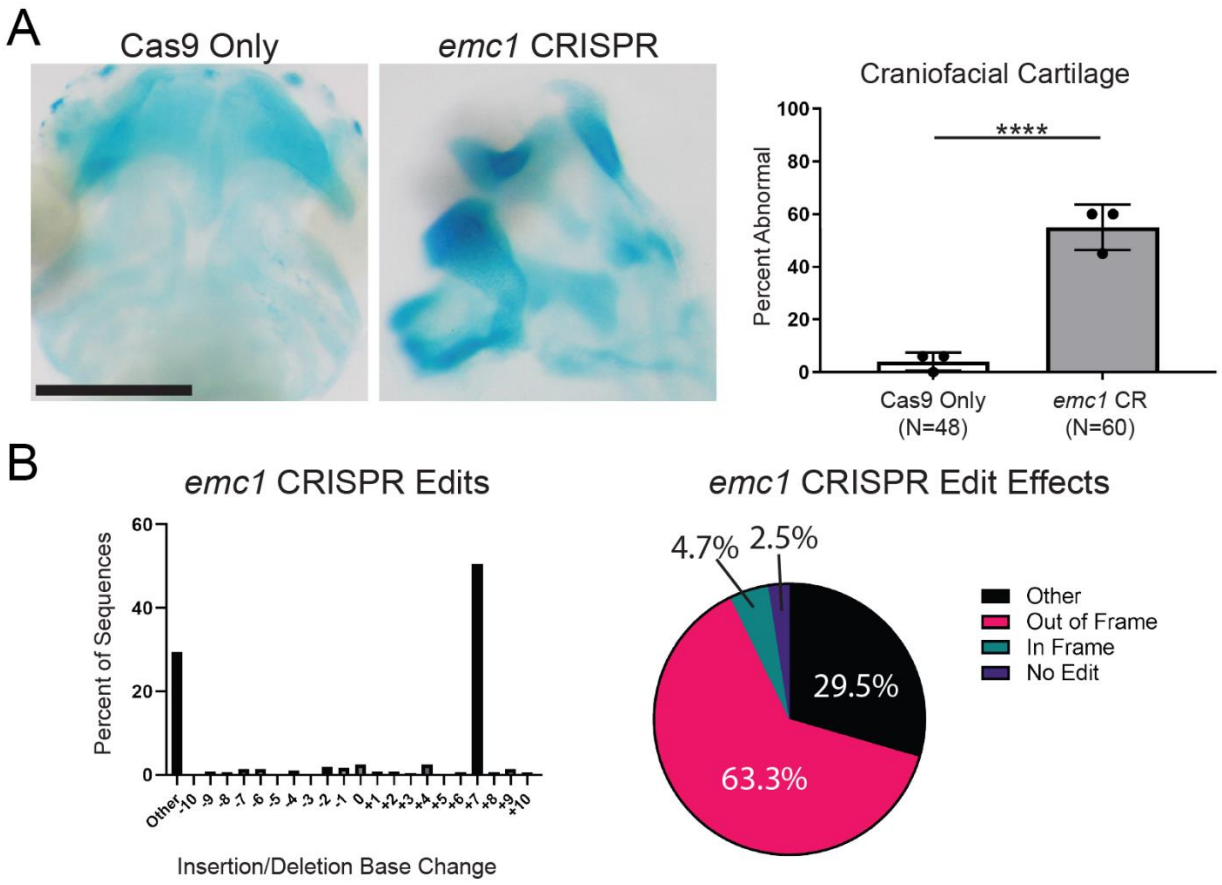

Supplemental Figure 2 F0 CRISPR mosaic knockout of *emc1* causes abnormal craniofacial morphology. **(A)** Representative images and quantitation of Cas9 only (n=48) and Cas9 + *emc1* sgRNA injected (n=60) stage 45 embryos stained with Alcian blue over 3 biological replicates. Scale bar indicates 250 μm. **(B)** Example TIDE analysis of insertion and deletion sizes along with their predicted effects in one embryo. This analysis of single embryos was carried out in 5 replicates to ensure consistent CRISPR mediated targeting. “Other” indicates changes that could not be analyzed via TIDE due to large size of indel. ****$p < 0.0001$ by Fisher’s exact test. Bars indicate mean and SD.

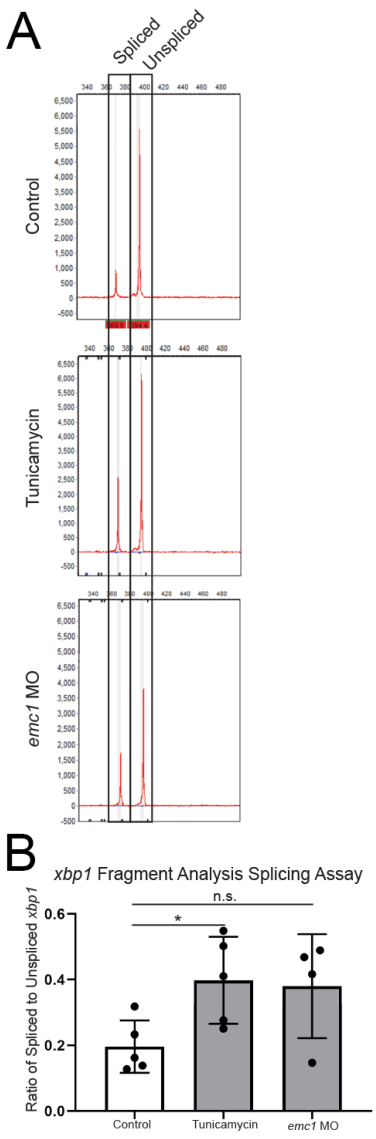

Supplemental Figure 3 Fragment analysis of *xbp1* splicing demonstrates increased endoplasmic reticulum stress in *emc1* morphants. **(A)** Examples of traces obtained from fragment analysis for *xbp1* spliced and un-spliced forms in 4-5 replicates of 30 pooled stage 24 control embryos, tunicamycin (positive control) treated embryos, and *emc1* morphant embryos. **(B)** Ratios of area under the curve measurements corresponding to peaks of spliced to un-spliced forms of *xbp1* in stage 24 control embryos, tunicamycin (positive control) treated embryos, and *emc1* morphant embryos demonstrate an increase in *xbp1* splicing in *emc1* morphants. *p<0.05 by Student's T-test. Bars indicate mean and SD.

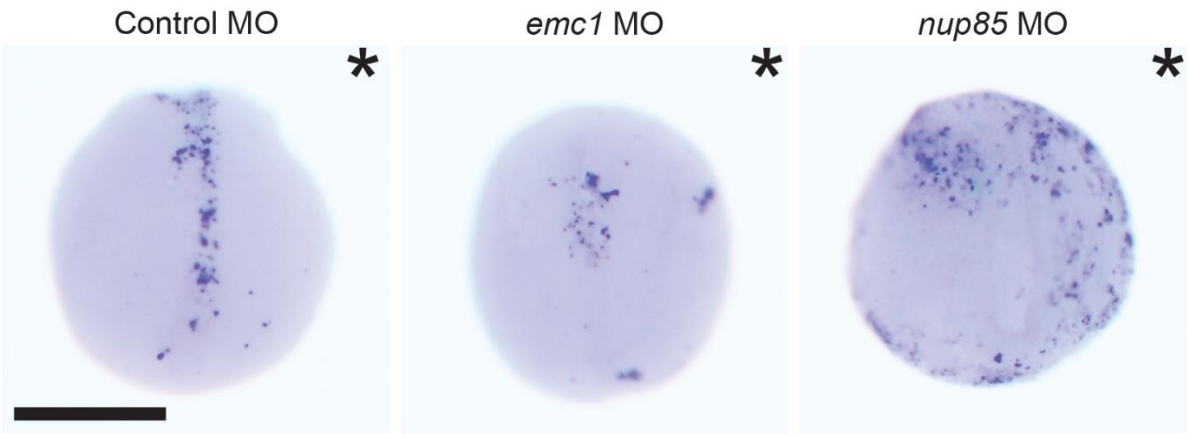

Supplemental Figure 4 TUNEL staining for cell death of St 20 embryos injected with MO in one cell at the two-cell stage. Representative images of embryos injected with control, *emc1*, or *nup85* MO affecting half of the embryo (indicated by asterisk side). Three replicates of 10 embryos were analyzed for each condition. Scale bar indicates 500 μm.

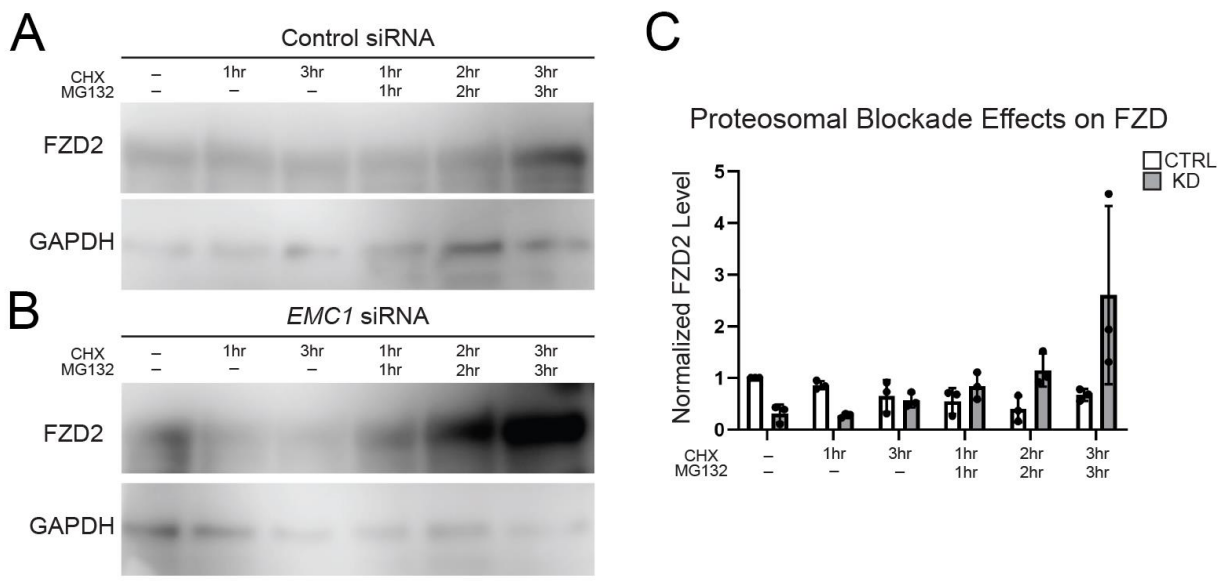

Supplemental Figure 5 Immunoblot analysis of FZD2 levels reveals proteasomal degradation as the source of FZD2 clearance in *EMC1* depleted RPE cells. **(A)** Immunoblot of FZD2 in cells transfected with a control siRNA and subjected to either cycloheximide treatment alone or cycloheximide and MG132 proteasomal inhibition performed in 3 biological replicates. **(B)** Immunoblot of FZD2 in cells transfected with *EMC1* siRNA and subjected to either cycloheximide treatment alone or cycloheximide and MG132 proteasomal inhibition performed in 3 biological replicates. **(C)** Normalized densitometry of FZD2 levels from immunoblot assays. Bars indicate mean and SD.

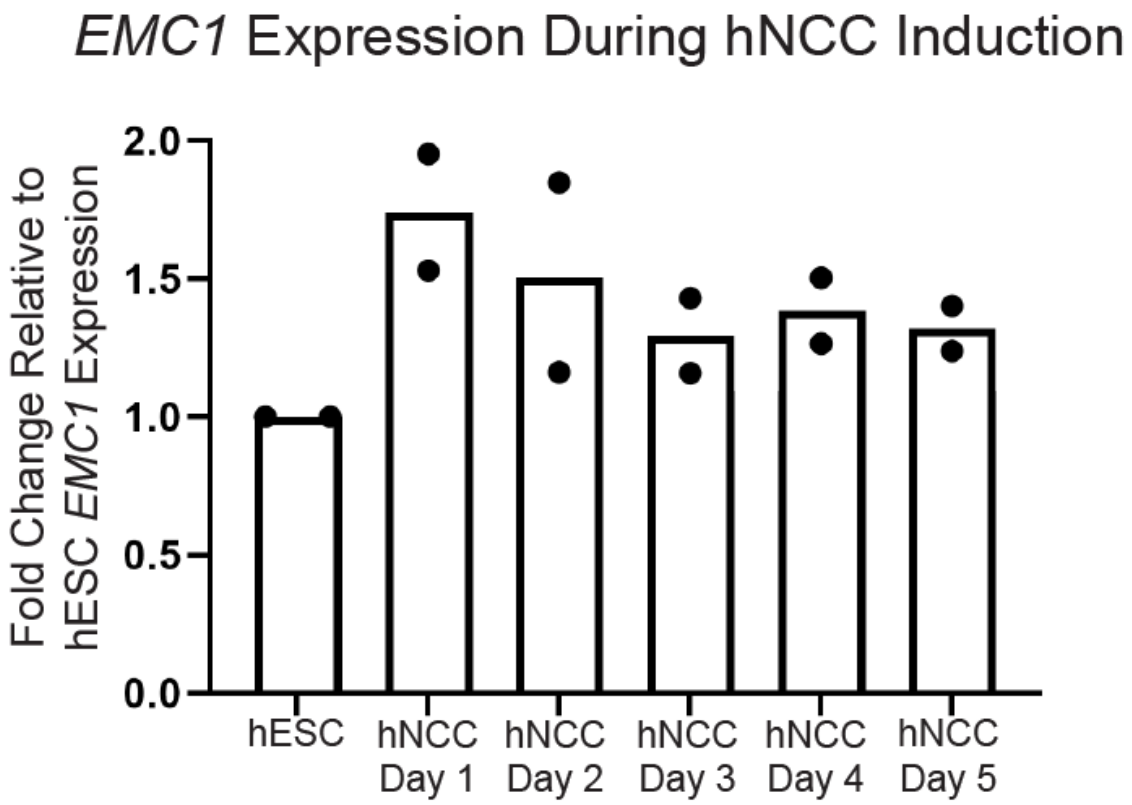

Supplemental Figure 6 *EMC1* expression during early human neural crest cell induction. qPCR analysis of *EMC1* transcripts during the human NCC induction protocol shows a sustained level of *EMC1* transcripts within one day after beginning induction for 2 biological replicates at each time point.

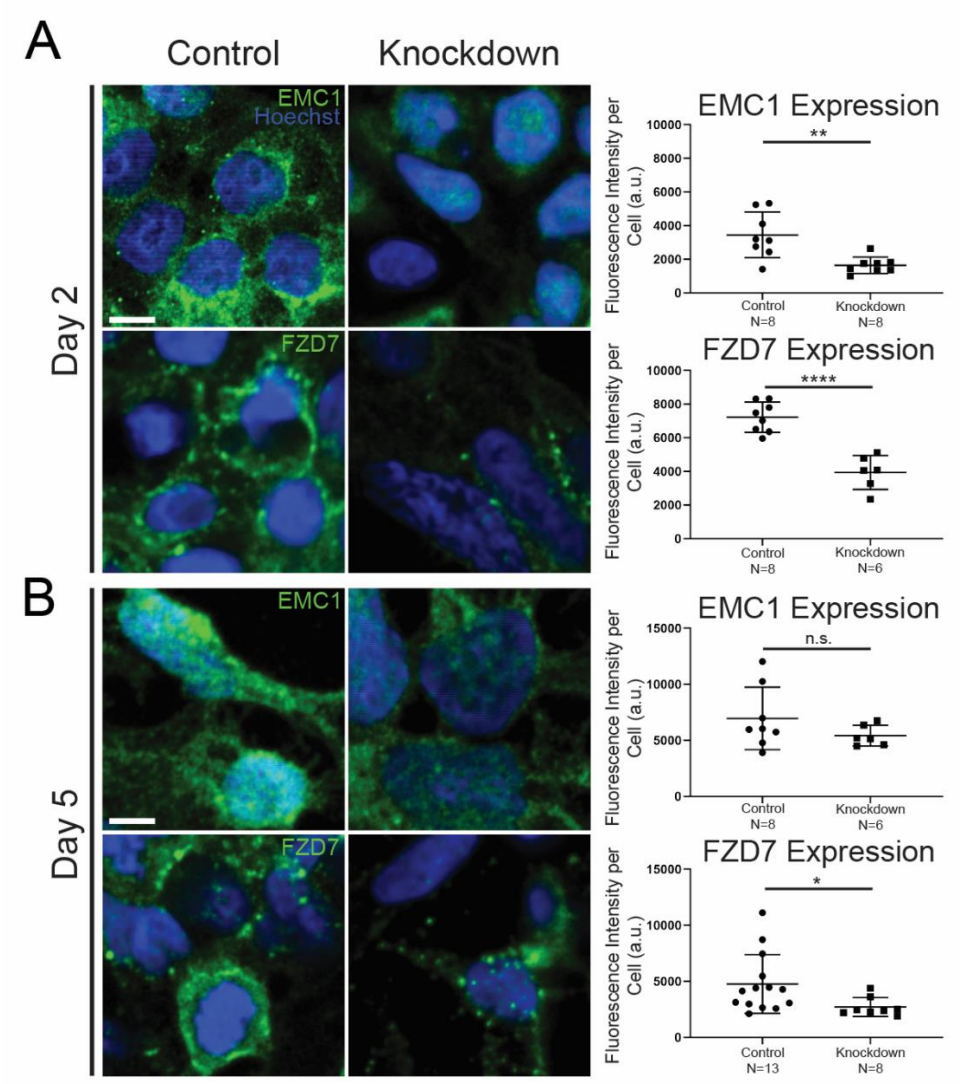

Supplemental Figure 7 *EMC1* knockdown via siRNA results in decreased FZD7 in hESC derived neural crest cells. **(A)** Immunofluorescence antibody labeling of EMC1 and FZD7 at day 2 of neural crest induction reveals a decrease in both as well as a more punctate appearance in residual FZD7 signal as compared to control siRNA treated cells. Cells in 3 replicates of 2-3 high power fields were assessed for each marker per condition. Scale bar indicates 5 μm. **(B)** Immunofluorescence antibody labeling of EMC1 and FZD7 at day 5 of neural crest induction reveals a recovery in EMC1 while FZD7 remains diminished and in a punctate pattern. Cells in 3 replicates of 2-4 high power fields were assessed for each marker per condition. Scale bar indicates 5 μm. Bars indicate mean and SD.

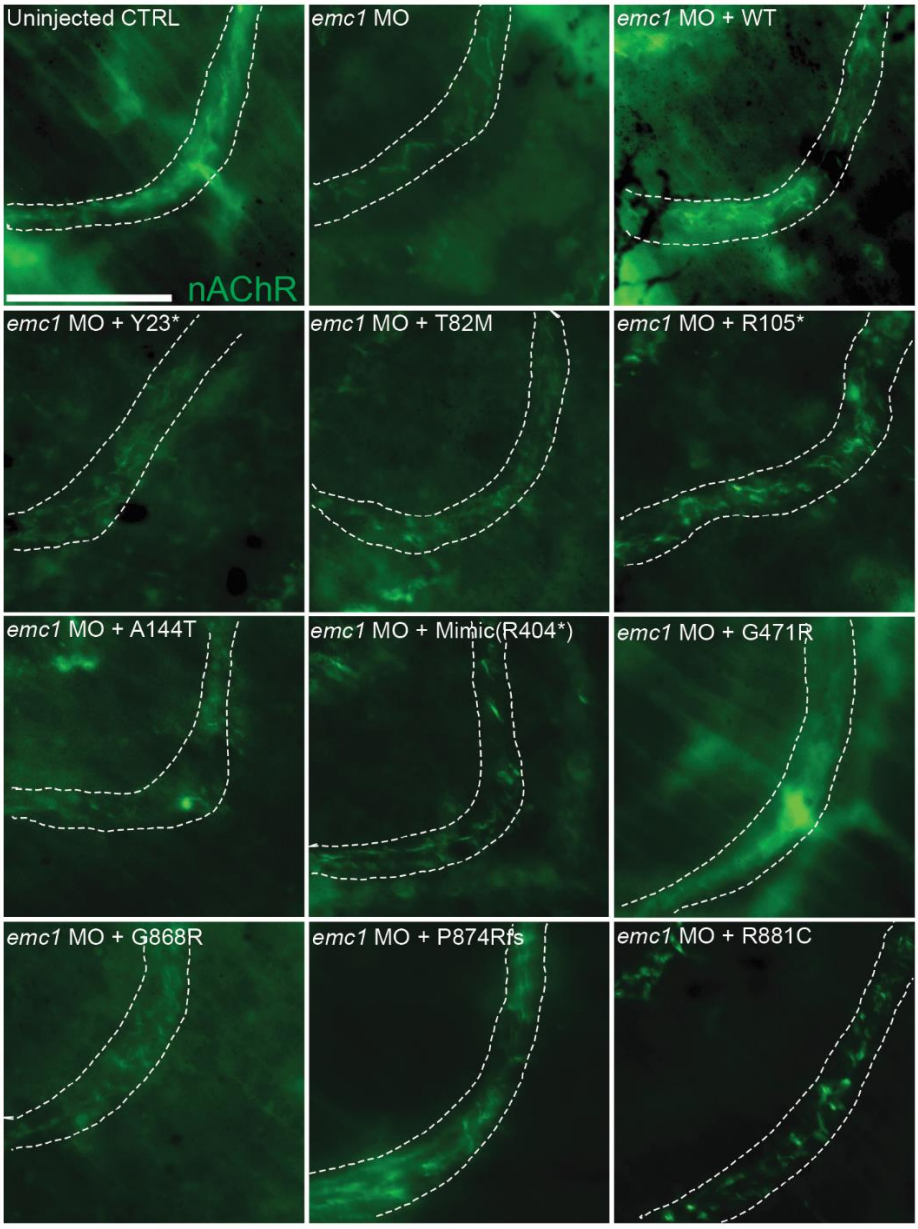

Supplemental Figure 8 Knockdown of emc1 in *Xenopus* results in abnormal nAChR signal in tail neuromuscular junctions that can be rescued through exogenous introduction of human *EMC1*. Injection of wildtype *EMC1* mRNA and to a lesser extent p.Gly471Arg (c.1411G>C) variant mRNA restores nAChR patterns of expression in *emc1* depleted tail neuromuscular tissue while mRNA of other variants do not. Three replicates of 8 embryos were analyzed for each condition. Scale bar indicates 50 μm. Images of uninjected control and *emc1* MO labeling of nAChR are from subregions of images shown in Figure 4C.

EMC1 Variant	Acquisition	Zygosity	Change in Coding Sequence	Change in Amino Acid Sequence	Effect	ExAC MAF	Source	Phenotype
chr1:19577935G>C	Inherited	Het	c.69C>G	p.Tyr23Stop	Stopgain	0	Jin et al 2017	Total Anomalous Pulmonary Vascular Return + Atrial Septal Defect
chr1:19577907A>T	Inherited	Het	c.96-2A>T	Unknown	Splice	0	Jin et al 2017	Transposition of the Great Vessels + Ventricular Septal Defect
chr1:19570485G>A	Inherited	Hom	c.245C>T	p.Thr82Met	Missense	0	Harel et al 2016	Global Developmental Delay
chr1:19570175G>A	Inherited	Het	c.313C>T	p.Arg105Stop	Stopgain	0	Jin et al 2017	Tetralogy of Fallot
chr1:19568918C>T	Inherited	Hom	c.430G>A	p.Ala144Thr	Missense	0	Abu-Safieh et al 2013	Retinitis Pigmentosa
chr1:19564510C>T	Inherited	Hom	c.1212+1G>A	Truncated protein after exon 11 product	Splice (premature stop)	0	Geetha et al 2017	Cerebellar Atrophy, Visual Impairment, Psychomotor Retardation with Epilepsy
chr 1:19561645C>G	De Novo	Het	c.1411G>C	p.Gly471Arg	Missense	0	Harel et al 2016	Global Developmental Delay
chr1:19547328C>T	Inherited	Hom	c.2602G>A	p.Gly868Arg	Missense	0	Harel et al 2016	Global Developmental Delay
chr1:19547308-19547311delAGGA	Inherited	Hom	c.2619_2622delTCCT	p.Pro874Arg*fs	Frame Shift	0	Harel et al 2016	Global Developmental Delay
chr1:19547289G>A	De Novo	Het	c.2641C>T	p.Arg881Cys	Missense	0.00002478	Homsy et al 2015	Bicommissural Aortic Valve

Supplemental Table 1 Previously identified *EMC1* variants.

qPCR Primers			
Gene	**Forward**	**Reverse**	**Species**
EMC1	AAAAAGGCAGATGGCTTGCTG	TCTTAATCTGACTCCGGGGCT	Homo sapiens
PAX3	GAACCCGGGCATGTTCAG	ACGGCACGGTGTTTCGA	Homo sapiens
PAX7	GCGACTCCGGATGTAGAGAA	ATCCTTCAGCAGCCTGTCC	Homo sapiens
SOX9	CCCCAACAGATCGCCTACAG	GAGTTCTGGTGGTCGGTGTAGTC	Homo sapiens
SNAI2	GATCCTCAGCTCAGGAGCATACA	GGAGTATCCGGAAAGAGGAGAGA	Homo sapiens
FOXD3	TCATCACCATGGCCATCCT	GGAAGCGGTTGCTGATGAAC	Homo sapiens
SOX10	GAGGCTGCTGAACGAAAGTGA	GCGGCCTTCCCGTTCT	Homo sapiens

rtPCR Primers			
Gene	**Forward**	**Reverse**	**Species**
xbp1	GACTGCTCGGGACAGGAAAA	GCCCAACAAGAGATCAGACTCA	Xenopus tropicalis

Antibodies	**Vendor**	**Catalog**	**Dilution**	**Species Raised In**
α-BUNGAROTOXIN (labeling of NAChRs) AF488	Thermo Fisher Scientific	B13422	1:1000	Bungarus multicinctus
EMC1	Thermo Fisher Scientific	PA5-23732	1:100 IF 1:1000 WB	Rabbit
FZD2	Abcam	ab109094	1:100 IF 1:1000 WB	Goat
FZD7	Abcam	ab64636	1:100 IF 1:1000 WB	Rabbit
PAX3	Developmental Studies Hybridoma Bank	Pax3	1:10	Mouse
PAX7	Developmental Studies Hybridoma Bank	Pax7	1:10	Mouse
RHO	Santa Cruz Biotechnology	sc-57432	1:200	Mouse
GAPDH	Novus Biologicals	NB600-502	1:1000	Mouse
HRP-β-ACTIN	Santa Cruz Biotechnology	sc-47778	1:30000	Mouse
AF488 anti-mouse	Life Technologies	A21200	1:1000	Chicken
AF488 anti-rabbit	Life Technologies	A21441	1:1000	Chicken
AF488 anti-goat	Life Technologies	A11055	1:1000	Donkey
HRP anti-mouse	Jackson ImmunoResearch	115-035-003	1:10000	Goat
HRP anti-rabbit	Jackson ImmunoResearch	111-035-003	1:10000	Goat
HRP anti-goat	Jackson ImmunoResearch	705-035-003	1:10000	Rabbit

Supplemental Table 3 Primer and Antibody Information